The Rostromedial Tegmental Nucleus (RMTg), a GABAergic Afferent to Midbrain Dopamine Neurons, Encodes Aversive Stimuli and Inhibits Motor Responses

Thomas C. Jhou,[1,*] Howard L. Fields,[2] Mark G. Baxter,[3] Clifford B. Saper,[4] and Peter C. Holland[5]
[1]Behavioral Neuroscience Branch, National Institute on Drug Abuse, Baltimore, MD 21224, USA
[2]Ernest Gallo Clinic and Research Center, University of California at San Francisco, Emeryville, CA 94608, USA
[3]Department of Experimental Psychology, University of Oxford, OX1 3UD Oxford, UK
[4]Beth Israel Deaconess Medical Center, Harvard University, Boston, MA 02215, USA
[5]Department of Psychological and Brain Sciences, Johns Hopkins University, Baltimore, MD 21218, USA
*Correspondence: tomjhou@gmail.com
DOI 10.1016/j.neuron.2009.02.001

SUMMARY

Separate studies have implicated the lateral habenula (LHb) or amygdala-related regions in processing aversive stimuli, but their relationships to each other and to appetitive motivational systems are poorly understood. We show that neurons in the recently identified GABAergic *rostromedial tegmental nucleus* (RMTg), which receive a major LHb input, project heavily to midbrain dopamine neurons, and show phasic activations and/or Fos induction after aversive stimuli (footshocks, shock-predictive cues, food deprivation, or reward omission) and inhibitions after rewards or reward-predictive stimuli. RMTg lesions markedly reduce passive fear behaviors (freezing, open-arm avoidance) dependent on the extended amygdala, periaqueductal gray, or septum, all regions that project directly to the RMTg. In contrast, RMTg lesions spare or enhance active fear responses (treading, escape) in these same paradigms. These findings suggest that aversive inputs from widespread brain regions and stimulus modalities converge onto the RMTg, which opposes reward and motor-activating functions of midbrain dopamine neurons.

INTRODUCTION

Decades of study have produced a wealth of information about brain systems that process aversive stimuli, particularly noxious or fear-eliciting stimuli (Brooks and Tracey, 2005; McNally and Westbrook, 2006). These aversive processes are believed to interact with appetitive motivational systems, though mechanisms of such interactions are poorly understood (Konorski, 1967; Dickinson and Dearing, 1979; Daw et al., 2002; Fields, 2007; Koob and LeMoal, 2008; Leknes and Tracey, 2008). A recent breakthrough in understanding these interactions has come from elegant studies by Hikosaka and colleagues showing that neurons in the lateral habenular nucleus (LHb), whose acti-

vation strongly inhibits dopamine (DA) neurons (Christoph et al., 1986; Ji and Shepard, 2007), are activated by aversive stimuli and reward omission and inhibited by reward-predictive cues or unexpected rewards (Matsumoto and Hikosaka, 2007, 2009; Geisler and Trimble, 2008). These "negative reward prediction errors" are inverse to firing patterns in putative dopaminergic midbrain neurons (Mirenowicz and Schultz, 1994, 1996; Hollerman and Schultz, 1998; Ungless et al., 2004; Pan et al., 2005; Coizet et al., 2006). Furthermore, LHb activation by reward omission precedes DA neuron inhibition (Matsumoto and Hikosaka, 2007), and LHb stimulation inhibits almost all midbrain DA neurons at short latency (Christoph et al., 1986; Matsumoto and Hikosaka, 2007; Ji and Shepard, 2007), suggesting a strong inhibitory influence of the LHb on DA neurons.

Despite much renewed interest, the mechanisms of habenula inhibition of DA neurons are not well understood. Direct LHb projections to the substantia nigra pars compacta (SNC) are sparse (Araki et al., 1988; Herkenham and Nauta, 1979; R. Matheson et al., 2008, Soc. Neurosci., abstract), and LHb efferents to the ventral tegmental area (VTA), while more substantial, are largely glutamatergic (S.R. Sesack, personal communication) and include many fibers of passage that continue caudally past the VTA (Araki et al., 1988). This strongly suggests an indirect influence of LHb on midbrain dopamine neurons (Hikosaka et al., 2008). In addition, aversive behaviors are influenced by numerous structures aside from the LHb. LHb lesions have no effect on fear-conditioned freezing in unstressed animals (Heldt and Ressler, 2006; Murphy et al., 1996), whereas lesions of the amygdala and its downstream targets in the ventral periaqueductal gray matter (PAG), markedly reduce fear-conditioned freezing (LeDoux et al., 1988; LaBar and LeDoux, 1996; Kim et al., 1993). Yet other measures of fear and anxiety are unaffected by amygdala lesions and depend instead on additional structures, such as the extended amygdala or septohippocampal systems (Treit and Menard, 1997; Fendt et al., 2003). Hence, the LHb, DA systems, and numerous other structures play distinct roles in mediating aversive behaviors, but how, or if, they interact is not known.

Recently, a novel GABAergic brain region, the *rostromedial tegmental nucleus* (RMTg), has been identified which could mediate the inhibitory effect of the LHb on midbrain DA neurons,
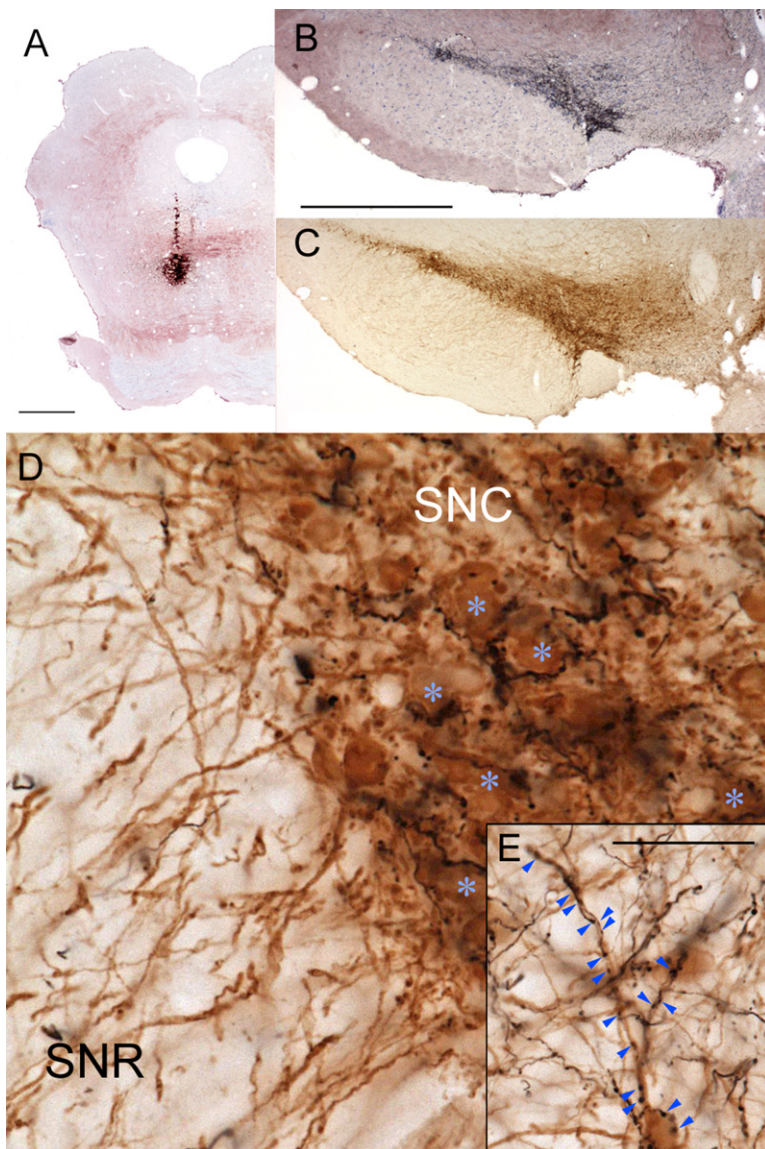
Figure 1. RMTg Efferents Appose Multiple Populations of Histochemically Identified Dopamine Neurons

A small injection of the anterograde tracer biotinylated dextran (BD) into the RMTg (A) produces massive numbers of labeled axons in the substantia nigra pars compacta (SNC) and ventral tegmental area (black label in [B]), shown against a Nissl counterstain. The density of BD labeling closely parallels the density of tyrosine hydroxylase-immunoreactive (TH-ir) soma in an adjacent section (brown label in [C]). In high-magnification photos of a separate case with a similar injection, anterogradely labeled fibers partly encircle TH-ir soma (blue asterisks) (D). Anterogradely labeled fibers are much less common in the substantia nigra pars reticulata (SNR), despite that region's abundant distal TH-ir dendrites. Anterograde projections also target TH-ir soma and dendrites in other dopamine fields, such as the retrorubral area (E, appositions indicated by blue arrowheads.). Scale bars in (A) and (B) are both 1 mm (bar in [B] also applies to [C]). Scale bar in (E) is 50 μm (also applies to [D]).

et al., 2007; Geisler et al., 2008; Jhou et al., 2009). Though this activation might suggest a role in reward, similar activation was not seen after morphine administration (Perrotti et al., 2005). Furthermore, psychostimulants activate both reward and stress-related brain systems (Swerdlow et al., 1993), making interpretation of their influence on the RMTg ambiguous.

Influenced by our anatomic findings, we examined the RMTg role in processing aversive and appetitive stimuli using physiological, anatomical, and behavioral techniques. We specifically examined whether RMTg neurons: project to histochemically identified DA neurons, preferentially respond to aversive stimuli and cues, are selectively activated by such stimuli over other afferents to the VTA, and modulate aversive behaviors mediated by distinct regions upstream from the RMTg. Some of the data in this study were previously shown in abstract form (T.C. Chou, M.G. Baxter, and C.B. Saper, 2004, Soc. Neurosci., abstract; due to name spelling change, Chou refers to T.C.J., the first author of the current work; T.C. Jhou and M.Gallagher, 2007, Soc. Neurosci., abstract).

while also integrating information from the extended amygdala and many other closely connected regions (Jhou, 2005; Jhou et al., 2009). This same region has also been identified by Barrot and colleagues, who have termed it the "tail of the VTA" (Kaufling et al., 2009). This nucleus occupies a column of tissue extending from the caudal edge of the ventral tegmental area (VTA), to the rostral edge of the cholinergic neurons of the pedunculopontine nuclei (PPTg). The RMTg also receives a strikingly focused afferent input from the LHb, and additional inputs from the extended amygdala and amygdala target regions such as the ventral PAG (Jhou et al., 2009; Kaufling et al., 2009). In turn, RMTg efferents project densely to midbrain regions where dopamine neurons are found (Jhou et al., 2009), and make inhibitory-type synapses onto VTA dopamine neurons (S.R. Sesack, personal communication). Little is known about the function of the RMTg, aside from its strong Fos activation by psychostimulants (Scammell et al., 2000; Perrotti et al., 2005; Colussi-Mas
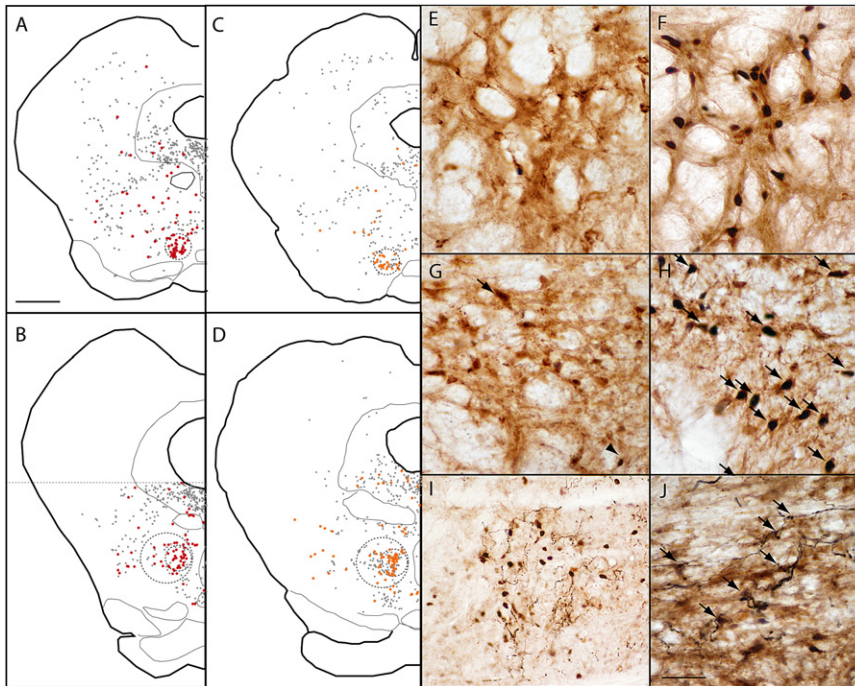
RESULTS

RMTg Efferents Appose Midbrain Dopamine Neurons

Previous work demonstrated intense RMTg projections to the VTA and substantia nigra pars compacta (SNC) (Jhou et al., 2009) but did not examine whether these projections appose histochemically identified DA neurons. Hence, we injected the anterograde tracers biotinylated dextran (BD) or phaseolus vulgaris-leucoagglutinin (PHAL) into the RMTg in five rats (Figure 1A) and then performed simultaneous histochemistry for anterograde tracer (Figure 1B) and tyrosine hydroxylase (TH) (Figure 1C). All cases showed numerous anterogradely labeled axons apposed to TH-immunoreactive neurons in all DA subfields, including the VTA, SNC (Figure 1D), central linear

Figure 2. VTA-Projecting Neurons in the RMTg, but Not Surrounding Areas, Coexpress GAD67 and Footshock-Induced Fos

(A–D) After retrograde tracer injections into the VTA, retrogradely labeled neurons are clustered in the RMTg but also found throughout the reticular formation (black and red filled symbols). Retrogradely labeled neurons coexpressing GAD67 (red symbols in [A]–[B]) are dense within the RMTg, as are retrogradely labeled neurons expressing shock-induced Fos (orange symbols in [C]–[D]). Colabeling in rostral (A and C) and caudal (B and D) levels is particularly high within the central "core" of the RMTg (smaller dashed circles), is less dense in the RMTg "periphery" (larger dashed circles in [B] and [D]) and is uncommon outside the RMTg. Photomicrographs of the RMTg from shocked (F) but not unshocked (E) rats show marked shock-induced Fos (black nuclei) in retrogradely labeled neurons (brown cytoplasmic label). Similarly, GAD67-immunoreactive neurons in the RMTg contain very little Fos in unshocked rats (G) but colocalize heavily with Fos after footshock presentation (H, arrows). After anterograde tracer injections into the medial portion of the lateral habenula (LHb), labeled fibers in the RMTg intermingle with shock-activated Fos nuclei (I), with less labeling where Fos nuclei are absent. In a separate case, labeled fibers arising from the LHb appose RMTg soma that are retrogradely labeled by a CTB injection into the VTA (J, arrows). Scale bar in (A) is 1 mm (applies to [A]–[D]). Scale bar in (J) is 250 μm (I) or 100 μm (E–H and J).

nucleus, and retrorubral fields (Figure 1E). Consistent with prior reports (Jhou et al., 2009), projections were roughly topographical, with more lateral and caudal injections producing high densities of labeled axons apposing more lateral DA neurons (Figure 1B), while medial and rostral injection sites produced more labeling in the VTA (not shown). In the SNC, anterogradely labeled fibers were often concentrated near DA soma, with single axons partly encircling individual DA neurons and making multiple appositions along the way (Figure 1D). Notably, anterogradely labeled fibers were conspicuously sparse in the SN pars reticulata (SNR), where DA soma were rare, despite that region's abundance of TH-immunoreactive dendrites (Figure 1D). Within the VTA, BD-labeled boutons frequently apposed TH-immunoreactive soma and dendrites, but some did not, suggesting that RMTg efferents also appose non-dopaminergic VTA neurons. Anterogradely labeled fibers were also substantial elsewhere in the brainstem, as previously reported (Jhou et al., 2009) but at lower densities than the projections to the DA subfields.
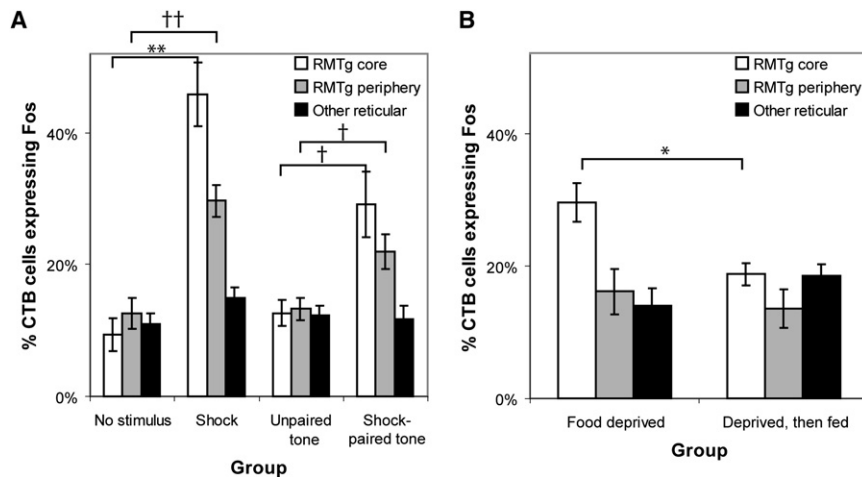
Conditioned and Unconditioned Aversive Stimuli Increase Fos in VTA-Projecting RMTg Neurons, Particularly Its Central Core

To determine the responses of VTA-projecting RMTg neurons to conditioned and unconditioned aversive stimuli, we placed retrograde tracer injections into the VTA of 24 rats, habituated all rats to test chambers, and then divided animals into four groups. On the test day, the first group received no stimulation (besides exposure to testing chambers), while the second received four footshocks (0.5 mA, 0.5 s each). A third group was given 2 days

of training over which 4 tones (55 dB, 2 kHz, 20 s duration) and 4 shocks were presented in explicitly unpaired fashion, followed by a third day of rehabituation to the chambers. On the test day, this group was then tested with tone presentation alone. The fourth group was trained in a similar manner, but with the tones and shocks explicitly paired, such that the four 20 s tones coterminated with the four 0.5 s shocks. This group was then tested with tone presentation alone, as in the third group. All rats were sacrificed one hour after session start. We discarded data from six rats in which retrograde tracer injections missed the VTA.

Because the RMTg lacks sharply delineated boundaries, we analyzed Fos-expressing cells separately in a "core" region located medially within the RMTg, where GABAergic VTA-projecting neurons are densest (Figure 2A; Jhou et al., 2009), and in a "peripheral" region around the midcaudal and caudalmost levels of the central core, where GABAergic retrogradely labeled cells are less dense, and intermingle with other cell types (Figure 2B; Geisler et al., 2008; Jhou et al., 2009). For the purposes of cell counts, we delineated the RMTg core using circles of diameter 500 μm centered at the region of highest density of retrograde labeling (smaller dashed circles, Figures 2A–2D). We delineated the RMTg periphery with 1 mm circles centered at the lateral edge of the core at its midcaudal and caudalmost levels (larger dashed circles in Figures 2B and 2D). This larger perimeter includes most GABAergic projections to the VTA (Figure 2B).

In the RMTg core, both footshocks and shock-predictive cues markedly increased Fos expression in retrogradely labeled neurons. In unstimulated rats, only 9.2% ± 2.2% (average ± SEM) of retrogradely labeled neurons were Fos immunoreactive

(n = 5; Figure 2E), whereas in footshocked rats (n = 5), 46% ± 5% of retrogradely labeled neurons were Fos-immunoreactive, a 5-fold increase (p < 0.001, two-tailed Student's t test, unequal variances; Figures 2C, 2F, and 3). In rats presented with explicitly unpaired auditory tones (n = 3), 13% ± 2% of CTB-labeled neurons were Fos-immunoreactive, which was not significantly different from the unstimulated group (p = 0.35), while among rats presented with shock-paired tones (n = 5), 30% ± 4% of CTB-labeled neurons in the central cluster expressed Fos, significantly higher than both the unpaired (p < 0.02) and unstimulated groups (p < 0.005).

The RMTg periphery exhibited similar effects, but of a smaller magnitude. Footshocks induced just over a 2-fold increase in Fos in VTA-projecting neurons in the peripheral RMTg relative to unshocked rats (p < 0.002), while shock-paired cues induced a roughly 70% increase in Fos in VTA-projecting neurons in the RMTg periphery relative to unpaired cues (p < 0.05; Figure 3A).

Outside the RMTg periphery, Fos expression in CTB-labeled neurons was not different between any of the four groups (p = 0.46, one-way ANOVA; Figure 3A).

Fos Activation in RMTg Core Is Concentrated in VTA-Projecting or GAD67-Expressing Neurons

Having analyzed Fos activation in VTA-projecting neurons, we next examined whether Fos-activation is specific to such neurons or also occurs in RMTg vicinity neurons not projecting to the VTA. For this analysis, we excluded rats in which the CTB injections did not fill the VTA, as they would have failed to retrogradely label RMTg neurons projecting to uninjected portions of the VTA. Across all 11 remaining rats, 85% ± 2% (average ± SEM) of Fos-expressing neurons in the RMTg central core contained retrograde tracer, a percentage that did not differ between the four groups (one-way ANOVA, p = 0.87). Furthermore, the relatively low numbers of Fos-expressing neurons that did *not* express retrograde labeling did not differ significantly between groups in either the RMTg core (p = 0.75) or periphery (p = 0.18). Hence, Fos modulations appear relatively confined to VTA-projecting neurons.

Although 75% of VTA-projecting neurons in the RMTg express GAD67 (Jhou et al., 2009), a minority do not; hence, we examined whether stimulus-induced Fos activation preferentially

occurs in GAD67-expressing neurons using double-label immunohistochemistry for GAD67 and Fos. Among eight rats in which immunohistochemistry was successful (two from each of the four groups), 79% ± 5% of Fos-expressing nuclei in the RMTg core were surrounded by GAD67-immunoreactive cell soma (Figures 2G and 2H), a percentage that did not differ across groups (ANOVA, p = 0.5).

Other Major Afferents to the VTA Lack Significant Fos Induction by Aversive Stimuli

The VTA receives widespread inputs from diverse brain areas (Geisler and Zahm, 2005), including several GABAergic regions (Tepper and Lee, 2007), so we next examined whether some of these regions are also modulated by shock stimuli or cues. We focused on regions particularly associated with affective processing: the nucleus accumbens, ventral pallidum, sublenticular area of the substantia innominata, lateral hypothalamic area, LHb, dorsal raphe/ventral PAG, and pedunculopontine nuclei (PPTg). Tissue from the nucleus accumbens and ventral pallidum was not available for the explicitly unpaired control group, so those two regions were only analyzed in the remaining three groups. Fos expression in all of these regions did not differ between available groups, though a nonsignificant trend could be seen in the LHb (ANOVA, p = 0.12 for LHb, p > 0.30 all other groups). One additional region that showed retrograde labeling after VTA injections was the medial tip of the substantia nigra pars reticulata (SNR). As this region overlapped the VTA injection site in many cases, we did not analyze it in depth, but in cases where CTB labeling was distinguishable, we noted conspicuous Fos induction after both shocks and shock-predictive cues in CTB-labeled cells that was not present in unstimulated rats. Hence, Fos induction by aversive stimuli or cues is not a general property of all VTA afferents but instead is confined to only a few afferents, most conspicuously the RMTg and possibly also the medial tip of the SNR.

Opposite Modulation by Appetitive versus Aversive Outcomes

Finally, we examined whether appetitive stimuli also affect Fos in RMTg VTA-projecting neurons. We placed retrograde tracers

into the VTA of two additional groups of rats, and food-deprived both groups to 85% of their initial body weight. Rats in one group, designated the "deprived" group (n = 4), were sacrificed after 60 min of exposure to behavioral chambers, while rats in the other group, designated the "fed" group (n = 5), were sacrificed after the same duration in the chambers but with ad libitum access to a highly palatable food. In the deprived group, 32% ± 2% of retrogradely labeled neurons in the RMTg central core expressed Fos, significantly higher than the unstimulated rats (p < 0.002; Figure 3B), indicating that food deprivation itself elevates Fos in these neurons. In the fed group (average consumption 10 ± 2 g), 18% ± 2% of CTB-labeled RMTg core neurons expressed Fos, significantly less than the deprived group (p < 0.02; Figure 3B), indicating opposite directions of modulation by food as compared to shock stimuli. Although reduced, Fos in VTA-projecting RMTg neurons after feeding was still higher than in unstimulated rats (p < 0.02), possibly due to the longevity of the Fos protein. In contrast to the RMTg core, Fos levels in VTA-projecting neurons in the RMTg periphery or outside the RMTg were not significantly affected by deprivation or feeding (p > 0.4 each comparison; Figure 3B).

Stimulus-Activated RMTg Neurons Receive Habenular Afferents

Because LHb projections are especially dense to RMTg regions exhibiting methamphetamine-induced Fos (Jhou et al., 2009), we examined whether LHb efferents show a similar relationship to neurons expressing shock-induced Fos. We placed injections of the anterograde tracer biotinylated dextran amine (BDA) into the LHb in two additional rats that also received footshocks 1 hr before sacrifice (4× 0.5 mA). We observed labeled fibers with a particularly high density in the same areas where shock-induced Fos-expressing nuclei were most dense (Figure 2I). In two more rats, BDA was injected into the LHb along with CTB injections into the VTA; anterogradely labeled fibers apposed a substantial number of retrogradely labeled RMTg neurons (Figure 2J), though we did not assess whether these neurons exhibited stimulus-induced Fos.

RMTg Responses to Positive and Negative Stimuli Occur at Short Latency

We next examined the temporal characteristics of RMTg responses to appetitive and aversive stimuli, in order to determine whether they resemble responses previously observed in the lateral habenula (Matsumoto and Hikosaka, 2007). We made electrophysiological recordings from the RMTg region in behaving rats trained to associate distinct auditory cues with a small sucrose solution (10%, 50 μl) or brief footshock (20ms, 0.2 mA). Using drivable electrode arrays we recorded from 1076 units in the midbrain tegmentum of 17 rats. To determine whether electrodes passed through the RMTg cell-dense core, we stained tissue from the implanted animals for the μ-opioid receptor, which prominently labels the medial and rostral portions of the RMTg (Jhou et al., 2009). To determine whether electrodes passed through the peripheral RMTg, where μ-opioid receptor immunostaining is weaker, we superimposed photographs of electrode tracks over photographs of GAD67-express-

ing VTA-projecting neurons obtained from a previous study (Jhou et al., 2009; Figures 4A–4C, gray symbols).

Of all recorded units, 33 resided within the RMTg core, while an additional 151 resided within the diffuse periphery. The remaining 892 units were located entirely dorsal, lateral, or ventral to the RMTg. To determine whether these units discriminated between cues at short latency, we compared unit firing rates during the 500 ms after sucrose-predictive cue onset versus firing rates in the 500 ms after shock-predictive cue onset. These comparisons showed a striking reversal between firing patterns in RMTg units versus units outside the RMTg. In the RMTg core, 55% (18/33) of recorded units showed significant differences in postcue firing rates between the two cues (p < 0.02, Mann-Whitney U test), and a majority (72%, or 13/18) of these cue-selective units showed higher firing rates after the shock-predictive cue than the sucrose-predictive cue (Figure 4). In the RMTg periphery and non-RMTg regions, similar fractions of units were cue selective (82/151 or 54%, and 407/892 or 46% respectively), but the proportion of such units showing preferential firing to the shock-predictive cue was 55% (29/55) and 21% (94/424), respectively, indicating a marked and progressive decline in aversive-cue preference at progressively farther distances from the RMTg core (Figure 4D). The differences in aversive cue-preference proportions were highly significant (p < 10^{-9}, chi-square test).

We next examined whether RMTg units have a particular electrophysiological signature. Background firing rates of units in the RMTg core averaged 20.2 ± 2.2 Hz, significantly higher than units entirely outside the RMTg (10.7 ± 0.4 Hz, p < 0.01, Mann-Whitney U test), while firing rates of RMTg periphery units (11.4 Hz) were not significantly different from units outside the RMTg (p = 0.3). Analysis of waveform shapes showed that RMTg core units had consistently narrow spike widths (116 ± 16 μs average ± standard deviation, measured peak-to-trough), while units in the RMTg periphery and outside the RMTg had significantly longer spike durations and much higher standard deviations (210 ± 85 and 188 ± 70 μs average ± standard deviation, respectively, p < 0.05). Although spike widths in the RMTg core were narrower than elsewhere, sucrose cue-selective and shock cue-selective unit spike widths did not differ from each other within the RMTg core, periphery or elsewhere (p > 0.5 each, Mann-Whitney U test).

RMTg Shock-Cue Preferring Units Are Modulated by USs in the Same Direction as CSs

In addition to CS responses, we also examined whether units responded to USs by comparing firing rates after sucrose or shock delivery with firing rates on "omission" trials in which these outcomes were omitted. Units were classified as "shock-activated" if they showed higher firing rates during the 500 ms after shock presentation than during the same period on shock-omission trials (p < 0.02, Wilcoxon signed-rank test). Similarly, "shock-inhibited" units were those that fired slower during the 500 ms after shock presentation than on omission trials. "Sucrose-activated" and "sucrose-inhibited" units were defined analogously. Omission trials were given in 10 of our 17 rats, accounting for 33 of RMTg core units, 71 of RMTg peripheral units, and 588 units overall.
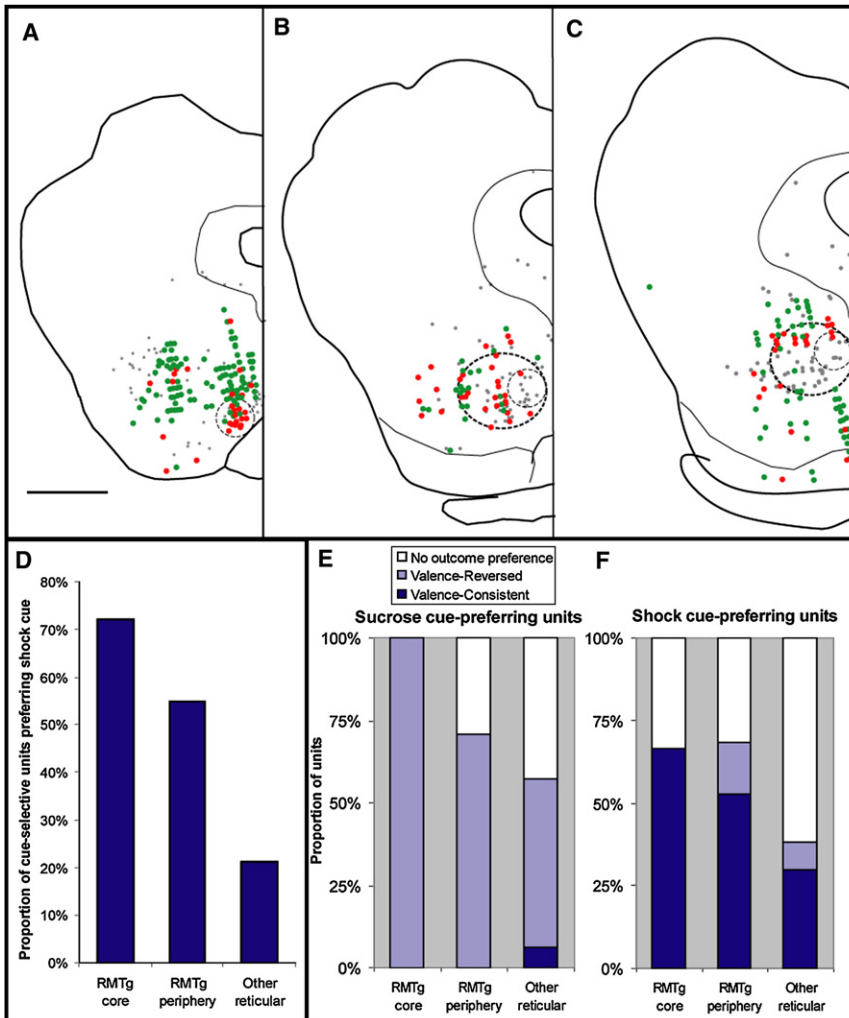
Figure 4. Extracellularly Recorded Neurons that Respond to Both Shock Cues and Shocks Are Concentrated in the RMTg

Electrophysiologically recorded units that preferred shock cues (red filled symbols) predominate in the RMTg "core" (small dashed circles, A–C), while sucrose-cue preferring units (green filled symbols) predominate outside the RMTg. The RMTg periphery (larger dashed circles, B and C), contains fewer shock-cue preferring units than the core but more than areas entirely outside the RMTg (D). Light gray filled symbols in (A)–(C) indicate locations of GAD67-expressing VTA-projecting neurons from an earlier report (Jhou et al., 2009). Sucrose-cue preferring units are predominantly valence-reversed, i.e., exhibit opposite modulation by cues and their associated outcomes (E, light blue bars), while shock cue-preferring units are predominantly valence-consistent, exhibiting similar directions of modulation by cues and their associated outcomes (F, dark blue bars). The RMTg core has the highest concentration of shock cue-preferring units (D), as well as the highest proportion of such units that also prefer the shock outcome (F), with both proportions declining progressively at farther distances from the core. Scale bar in (A), 1 mm.

We further classified recorded units as "valence-consistent" if they were activated by the US predicted by that unit's preferred CS, or inhibited by the opposite US, or both. Conversely, units were "valence-reversed" if they were excited by the US *not* predicted by the unit's preferred CS, and/or *inhibited* by the US predicted by the preferred CS (or both). Units were deemed to have no clear outcome preference if they responded to neither outcome, or responded in the same directions to both outcomes.

In the RMTg core, most (8/12 or 67%) shock-cue preferring units were valence consistent (Figure 4F), that is, they were activated by shock and/or inhibited by sucrose, while the remainder had no outcome preference. In the RMTg periphery, a somewhat lower proportion (10/19 or 53%) of shock-cue preferring units were valence consistent, while a few units (3/19 or 16%) were valence-reversed, and the remaining (6/19 or 32%) lacked an outcome preference (Figure 4F). In the reticular formation outside the RMTg, shock-cue preferring units were much less likely to be valence-consistent (14/52 or 27%), as most of these units simply lacked an outcome preference (34/52 or 65%), and valence-inconsistent units again accounted for only a small proportion (4/52 or 8%). Hence, RMTg units, and especially

RMTg core units, were distinguished not only by their high likelihood of preferring the shock-predictive cue, but also by their higher likelihood of being shock activated and/or sucrose inhibited.

In contrast, sucrose cue-preferring units both inside and outside of the RMTg were predominantly valence reversed (Figure 4E, with example unit in Figure 5D). In the RMTg core all (5 of 5) sucrose cue-preferring units were valence reversed, that is, activated by shock and/or inhibited by sucrose, while in the RMTg periphery, a majority (14/20 or 70%) of sucrose cue-preferring units were valence-reversed and the remainder showed no outcome preferences. Outside the RMTg, 66/129 or 51% of sucrose cue-preferring units were valence reversed, while a few (8/129 or 6%) units were valence-consistent, and the remaining (55/129 or 43%) units had no outcome preference (Figure 4E).

Interestingly, shock-cue preferring units in the RMTg core invariably had fast phasic responses to shock-predictive cues, typically responding within 100 ms (Figures 5A and 5B), while the RMTg periphery exhibited a mixture of units with fast phasic responses, and others with slow ramping firing rate increases that evolved over several hundred milliseconds (Figure 5C).

Reward Omission Responses
LHb neurons in primates are excited not only by aversive stimuli, but also by unexpected reward omission (Matsumoto and Hikosaka, 2007, 2009), consistent with temporal difference learning models (Sutton and Barto, 1998; Montague et al., 1996). In
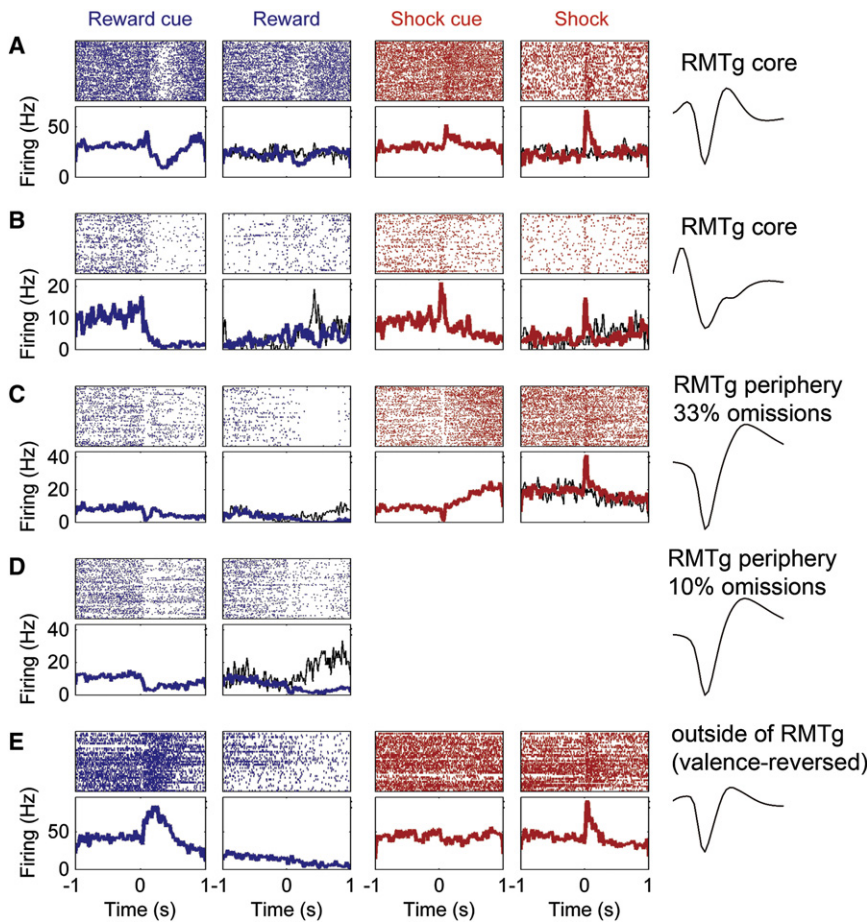
Figure 5. RMTg Units Respond to Cues and Outcomes at Short Latency, and Some Are Phasically Activated by Reward Omission

Many units in the RMTg core (A and B) were phasically inhibited by sucrose-predictive cues and sucrose (columns 1–2), and excited by shock-predictive cues and shocks (columns 3–4). Raster-plots (top subpanels) and perievent spike-histograms (bottom subpanels) for each recorded unit are time-aligned to onset of cue or outcome. Some units also showed excitation by reward omission (B, thin black trace in column 2). Such omission responses were not seen when cue durations were randomized, thus making reward delivery time unpredictable (A, thin black trace in column 2). RMTg core units showed rapid basic excitations to shock-predictive cues, while some units in the RMTg periphery showed slow ramp-like excitations to these cues (C, column 3). Although the unit in (C) shows a transient inhibition to the shock cue, this inhibition also occurs to the sucrose cue, whereas the subsequent ramp-like increase is only seen after the shock cue. Unit in row (D) is the same unit as (C) but after omission probability was reduced from 33% to 10%, causing omission responses to become conspicuous (black trace in second column). Units outside the RMTg predominantly showed greater excitation to the sucrose-predictive cue than the shock-predictive cue (E, columns 1 versus 3). Such units often preferred the sucrose cue and the shock outcome; i.e., were "valence-reversed." Waveform traces are each 800 μs long.

many of our sessions, cue durations were randomized in a 1–3 s range, making it impossible for the rat to precisely determine the time of expected outcome. RMTg units recorded from these sessions never showed changes in firing rates after reward omission, relative to the immediately preceding 500 ms. However, nine rats were trained and tested using fixed 2 s cue durations. These sessions yielded a total of 46 cue-selective units in the RMTg core or periphery, and 159 from outside the RMTg. Among RMTg core/periphery units, 12/46 (26%) showed excitations by reward omission (Figures 5B and 5D), as defined by significantly higher firing rates during the 0.5 s after expected reward delivery time relative to the preceding 0.5 s (and higher firing rates on omission than rewarded trials; $p < 0.05$, Wilcoxon signed-rank test). In contrast, among units outside the RMTg area, only 5/159 (3%) showed excitations by reward omission, a significantly lower proportion than in the RMTg area ($p < 5 \times 10^{-9}$, chi-square test). Interestingly, excitations by reward omission were evident in both sucrose cue-preferring and shock cue-preferring RMTg units (7/23 and 5/23, respectively). Omission probability was fixed in most sessions at 33%, but in one session we manipulated the reward probability and noted a cue-selective unit that showed significant excitations to reward omission when the omission probability was 10% ($p < 0.05$; Figure 5D), but not when it was 33% (Figure 5C), consistent with temporal difference models which predict that outcome omission should elicit larger

responses when omissions are rarer, and hence more surprising (Sutton and Barto, 1998).

Comparison with Motor Behavior

Although observed RMTg firing patterns are consistent with encoding of affective valence, the midbrain also contains neurons mediating motor behaviors, such as attentional orienting (Holstege, 1991). Hence, we also examined whether RMTg firing patterns might reflect such task-related motor activity. Computer analysis of digitized session video showed that motor activity increased rapidly just after the sucrose-predictive cue (when rats approach the reward receptacle) whereas locomotion tended to decrease during consumption. As many RMTg units responded with inhibitions to both sucrose cues and sucrose, they are not likely to be reflecting motor activation alone. Conversely, motor activity after shocks tended to show large increases (startle), while shock-predictive cues tended to show modest decreases in locomotion (sometimes preceded by a brief excitation), reflecting freezing and orienting responses. Again, the similarity of many RMTg unit responses to shock cues and shocks contrasts with the very divergent motor responses to these stimuli.

RMTg Lesions Impair Passive Aversive Behaviors

Dopamine depletion impairs active behaviors such as escape, while enhancing passive aversive behaviors such as freezing
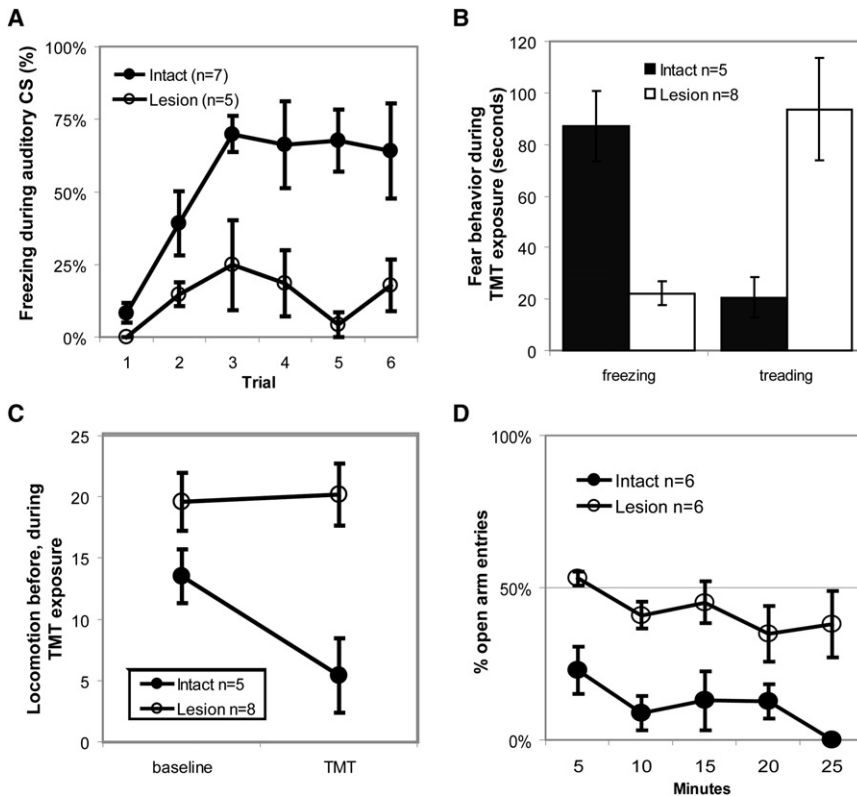
Figure 6. RMTg Area Lesions Markedly Impair Passive but Not Active Behavioral Responses to Fear-Inducing Auditory and Olfactory Stimuli

(A) RMTg area lesions markedly reduced freezing to a conditioned auditory tone. (B) Lesions reduced unconditioned freezing to the predator odor trimethylthiazoline (TMT), while increasing defensive treading/burying to a similar degree. Lesions did not affect locomotor activity during a 10 min baseline period before odor presentation, but abolished subsequent odor-induced loco-motor suppression (C). RMTg lesioned rats placed on a elevated plus maze made an equal number of entries into open versus closed arms (D), unlike controls which strongly avoided open arm entries. Notably, lesioned animals still spent less time in the open arms, indicating preservation of escape behavior, despite impairment of avoidance. All error bars indicate one standard error of the mean.

(Lenard and Beer, 1975). To examine whether the RMTg also modulates these types of aversive behaviors, we made fiber-sparing lesions of the RMTg region using the excitotoxin ibotenic acid, and then tested lesioned and unlesioned rats on three measures of anxiety and fear: auditory conditioned freezing, freezing to the predator odor trimethylthiazoline (TMT), and elevated plus maze arm avoidance. These behaviors were chosen because they depend on distinct forebrain systems, namely the amygdala, bed nucleus of the stria terminalis (BNST), and lateral septum, respectively (LaBar and LeDoux, 1996; Fendt et al., 2003; Treit and Menard, 1997). In conducting these tests, we attempted, where possible, to analyze both passive (avoidance, freezing) and active (escape, burying) responses.

We first examined conditioned freezing in five rats with lesions encompassing both the core and periphery of the RMTg (see Figure S1 available online). We also tested four saline-injected shams, and three unoperated rats. All rats were presented six pairings of a low amplitude (80 dB) 20 s auditory tone coterminating with an extremely loud (120 dB) 1 s tone US.

Saline-injected rats and unoperated control rats rapidly acquired conditioned freezing to the low-amplitude tone. Freezing levels did not differ between these two control groups (p > 0.5), and hence we pooled them into a single control group. In contrast, RMTg-lesioned rats, which had 73% ± 10% fewer Nissl-stained neurons in the RMTg region than controls, froze 76% ± 13% less than controls during the final 4 cue presentations (Figure 6A). Both lesioned and unlesioned rats showed startle responses to the US, indicating that these responses were relatively unaffected by RMTg lesions despite the large reductions in freezing.

We next examined the RMTg role in unconditioned freezing to the predator odor TMT, a behavior that is dependent on the BNST and medial amygdala, but not on the lateral amygdaloid regions involved in conditioned fear (Fendt et al., 2003; Müller and Fendt, 2006). Additional groups of ten lesioned and five saline-injected rats were exposed to 20 µl of the predator odor TMT in their homecage for 10 min sessions, preceded by a 10 min baseline period. Subsequent counts of Nissl-stained neurons revealed that 8 of the 10 lesioned animals had RMTg area cell loss exceeding 70%, with an average reduction of 82% ± 4% (Figure S2), while the remaining 2 animals ("partial lesion" rats) had less than 70% loss of RMTg area neurons, and were excluded from the lesioned group. Unlesioned control rats froze 87 ± 14 s during the 10 min exposure to TMT, while lesioned rats froze 22 ± 5 s, a 74% reduction (p < 0.01; Figure 6B). Lesioned rats also had marked increases in a stereotyped behavior variously referred to as "defensive treading" or burying, characterized by rapid forepaw thrusting directed forward toward an offending stimulus, often burying it entirely (Treit and Pinel, 2005; Owings and Morton, 1998, as reproduced in Reynolds and Berridge, 2001, Figure 1B). Whereas sham rats exhibited defensive burying for only 18 ± 9 s during the test period, RMTg lesioned rats engaged in this behavior for 101 ± 22 s, a 467% increase (p < 0.01; Figure 6B). The combined time spent freezing and treading did not differ between groups (105 ± 14 s for unlesioned, and 118 ± 21 s for lesioned rats, p > 0.4), indicating that the large reductions in freezing were compensated by roughly equal increases in treading.

Both sham and lesioned rats showed only low levels of freezing and defensive burying (<10 s each) during the 10 min baseline period before TMT presentation; these levels did not differ between lesioned and control groups (p > 0.07 both behaviors).

Though lesioned rats showed relatively little freezing to TMT, we still wondered if lesions affected motor responses to TMT to
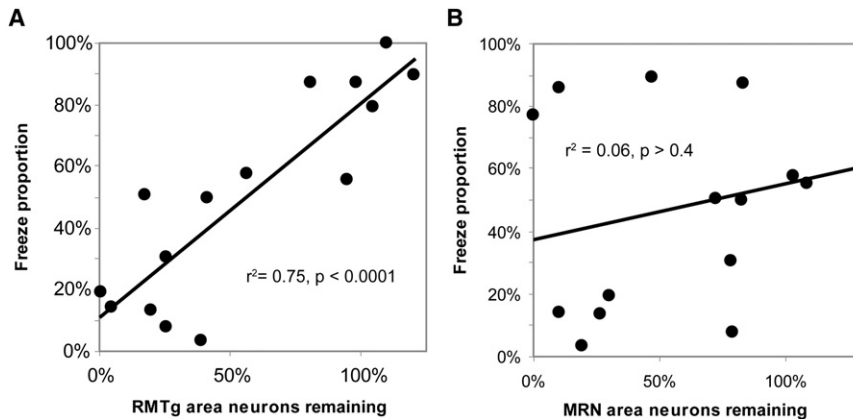
Figure 7. Deficits in Freezing to Predator Odor Correlate with Loss of Neurons in the RMTg but Not in the Nearby Median Raphe Nucleus (MRN)

Loss of RMTg area neurons correlates with reductions in predator odor-induced freezing as a proportion of total defense behavior (freezing + treading) (A), while loss of neurons in the adjacent median raphe nucleus (MRN) does not (B).

a lesser degree than required to produce outright immobility and freezing. Hence, we examined locomotor activity by counting cage midline crossings. During the 10 min baseline period, RMTg lesioned rats showed marginally higher activity levels than unlesioned rats, which did not reach statistical significance (p = 0.1; Figure 6C). During the 10 min TMT presentation, unlesioned rats showed 60% less locomotor activity than in the preceding baseline period (p < 0.05), while activity in lesioned rats remained unchanged from the baseline levels (p > 0.5; Figure 6C). Hence, RMTg area lesions blocked not only freezing responses, but also more general locomotor reductions induced by TMT.

Lesions targeted to the RMTg caused varying levels of damage to the adjacent median raphe nucleus (MRN), which has been implicated in fear and anxiety behaviors including freezing (Avanzi et al., 1998). However, across all 15 lesioned, unlesioned, and partially lesioned rats, we saw no correlation between the number of remaining MRN neurons and TMT-induced freezing as a fraction of total defense behavior (freezing + treading; p = 0.4; Figure 7B), nor with absolute durations of freezing (p > 0.6) nor defensive treading (p > 0.3). In contrast, the number of remaining RMTg neurons correlated strongly with freezing proportion (p < 0.0001; Figure 7A), as well as absolute durations of freezing (p < 0.001) and treading (p < 0.01).

Elevated Plus Maze

Finally, we examined whether RMTg lesions affect open-arm avoidance on an elevated plus maze having two open arms and two closed arms. This avoidance behavior is not affected by lesions of either the amygdala or BNST but is abolished by lesions of the septum (Treit and Menard, 1997; Pezuk et al., 2008), even though septal lesions do not diminish some other measures of fear (Sparks and LeDoux, 1995). In six unlesioned rats, only 14% ± 6% of all entries were into the open arms, a number significantly below 50% chance (p < 0.005; Figure 6D). In contrast, six lesioned rats made 45% ± 3% of all entries into the open arms, higher than the controls (p < 0.005), and not significantly different from chance (p = 0.2). Importantly, lesioned rats still spent much less time overall on the open than closed arms (237 ± 50 s versus 681 ± 162 s, p < 0.05), indicating that they still exited the open arms more rapidly than the closed arms, despite their failure to avoid the initial arm entry.

DISCUSSION

Anatomical studies have recently elucidated a major GABAergic structure in the midbrain reticular formation, termed the RMTg, which integrates a predominant input from the LHb with afferents from the extended amygdala and related regions and sends major outputs to midbrain DA fields, with additional projections to brainstem targets including major ascending arousal systems (Jhou, 2005; Jhou et al., 2009; Kaufling et al., 2009). We found convergent anatomical, physiological, and behavioral evidence that RMTg neurons encode aversive stimuli and promote passive aversive responses. In particular, single-unit recordings showed that many RMTg neurons are phasically activated by aversive conditioned or unconditioned stimuli, and also reward omission, and inhibited by appetitive conditioned or unconditioned stimuli. These patterns were similar to those reported for the LHb and inverse to the reward-predictive encodings of putative DA neurons. Furthermore, aversive cue-responsive RMTg units were also much more likely to respond to the shock outcome than the sucrose outcome, indicating similar directions of modulation by aversive cues and outcomes. In contrast, sucrose cue-preferring units tended to show opposite directions of modulation by cues and outcomes. Double-labeling experiments using Fos as a measure of neuron activity showed that RMTg neurons activated by aversive stimuli were largely VTA-projecting and GABAergic.

Convergence of Affective Functions from Habenula and Amygdala Target Structures

We found that the RMTg region exhibited a combination of properties that appear separately in many distinct regions upstream from it. RMTg phasic excitations by aversive stimuli and reward omissions resemble those of its LHb afferents (Matsumoto and Hikosaka, 2007), and the loss of inhibitory behaviors observed after our RMTg lesions are consistent with prior reports that LHb lesions increased locomotor activity (Murphy et al., 1996) and increased premature responding in a five-choice serial reaction time task (Lecourtier and Kelly, 2005). However, LHb lesions do not replicate the marked freezing deficits of RMTg lesions (Murphy et al., 1996; Heldt and Ressler, 2006), and RMTg lesion effects on freezing more closely resemble lesions of the ventrolateral PAG (LeDoux et al., 1988; Kim et al., 1993), another major afferent to the RMTg (Jhou et al., 2009). The ventrolateral PAG in turn receives major inputs from both the central nucleus of the amygdala (Hopkins and Holstege, 1978) and the BNST (Holstege et al., 1985), and so it is notable that RMTg lesions markedly

impaired freezing to conditioned auditory tones, a behavior which depends on the central and lateral amygdaloid nuclei (Lee et al., 2005), and also impaired unconditioned freezing to the predator odor TMT, which instead depends on the BNST and medial amygdala (Fendt et al., 2003). RMTg lesions also abolished open arm avoidance on an elevated plus maze, a behavior unaffected by amygdala or BNST lesions, but instead abolished by lesions of the septum (Treit and Menard, 1997; Pezuk et al., 2008), another region directly afferent to the RMTg, though indirect pathways may also be significant (Jhou et al., 2009). Furthermore, septal lesions do not reduce, and may even enhance, fear measures such as burying and conditioned freezing that are markedly affected by amygdala and BNST lesions (Sparks and LeDoux, 1995). Hence, the behavioral deficits observed after RMTg lesions appear to be triply dissociated among forebrain regions that may reside upstream from the RMTg.

While combining some properties of its hypothesized upstream afferents, the RMTg does not exhibit all of them. For example, electrophysiological recordings from the amygdala show a mixture of neurons encoding positive and negative valence (Saddoris et al., 2005; Paton et al., 2006), whereas positive valence encoding was nearly absent in the RMTg. Also, lesions of the amygdala, lateral septum, or BNST often impair both active and passive fear responses (Sparks and LeDoux, 1995; Schulz and Canbeyli, 2000; Treit and Menard, 1997), while our RMTg area lesions selectively impaired responses involving reductions or withholding of motor activity (freezing and avoidance) and spared or enhanced active responses (startle, open-arm escape, treading). The RMTg thus appears particularly specialized for representing negative stimuli and for promoting inhibitory behavioral responses to them. Furthermore, the RMTg plays these roles over a remarkably wide range of stimulus modalities and behavioral paradigms. These roles are inverse to those of DA depletion, which enhances freezing responses to fearful stimuli at the expense of escape responses (Lenard and Beer, 1975).

Anatomic Specificity of RMTg Function

The RMTg lacks sharp nuclear boundaries in Nissl stained material, and has only recently been defined as a collection of VTA-projecting neurons that express GAD67 (Jhou, 2005; Jhou et al., 2009; Kaufling et al., 2009) or Fos activation by amphetamine (Geisler et al., 2008). Despite the region's diffuse boundaries, we saw striking convergence of numerous neuronal response properties that were most prominent in the medial cell-dense "core" of the RMTg, less prominent in a lateral and caudal "peripheral" region, and absent or reversed outside the RMTg.

Our lesion experiments also showed that several aversive behaviors are critically dependent on neurons in the RMTg area. However, because lesions involved both the RMTg core and periphery and also spread somewhat outside the RMTg, we cannot rule out the possibility that behavioral deficits were due to loss of cells just outside the RMTg, or intermingled with the RMTg periphery. However, several factors argue for at least some behavioral contribution from RMTg GABAergic afferents to DA neurons. First, RMTg lesions induced behavioral effects that were opposite to those seen after DA depletion, as noted above. Second, Fos levels in RMTg core or periphery neurons *not* projecting to the VTA were not affected by shocks or shock-predic-

tive cues, suggesting these aversive stimuli preferentially influence VTA-projecting neurons. Third, lesion encroachment outside the RMTg region was most frequent dorsally and medially, but the region dorsal to the RMTg consists largely of decussating fibers (which are spared by excitotoxins), while damage to the MRN just medial to the RMTg was not correlated with altered behavioral responses to TMT. The lack of behavioral correlation with MRN damage is notable because several studies had implicated the MRN in similar functions as the RMTg, including inhibition of nucleus accumbens DA release (Wirtshafter and Trifunovic, 1992) and conditioned freezing to contextual cues (Avanzi et al., 1998). However, those studies did not distinguish the MRN from the adjacent RMTg, and because the MRN contains very few GABAergic projections to the VTA (Figure 2, also Jhou et al., 2009) and did not regulate responses to TMT, results from previous studies could have been mediated by the RMTg instead.

Not only is RMTg function distinguishable from surrounding midbrain structures, it is also distinct from VTA afferents arising elsewhere in the brain. We examined stimulus-induced Fos in VTA-projecting neurons in the PPTg, dorsal raphe, substantia innominata, and lateral hypothalamus, as well as GABAergic afferents from the nucleus accumbens, ventral pallidum, and SNR. Only the medial-most tip of the SNR showed Fos activations by shocks or shock-predictive stimuli, while the other structures did not.

Relationship to the Posterior VTA

Current findings place in context recent anatomic studies noting enigmatic "ball-like nuclei" (Olson and Nestler, 2007) in the posterior VTA that exhibit psychostimulant-induced Fos expression (Scammell et al., 2000; Perrotti et al., 2005), high levels of GAD67 (Olson and Nestler, 2007), and projections to other dopaminergic neurons (Ferreira et al., 2008). These studies variously designated this region as the "retroVTA," "posterior tail" of the VTA, or "caudal pole" of the VTA, but this region is now recognized as the rostral tip of the much larger RMTg structure (Jhou et al., 2009; Kaufling et al., 2009). In parallel with the anatomic studies of the caudal VTA, numerous reports show very different propensities for drug self-administration into the caudal versus rostral VTA. For example, GABA-A agonists are most readily self-administered into the posterior VTA (Ikemoto et al., 1998) while GABA-A *ant*agonists are more readily self-administered into the anterior VTA (Ikemoto et al., 1997). This parallels another finding that CREB upregulation in the caudal VTA makes cocaine more aversive, while the same manipulation in the rostral VTA makes cocaine more rewarding (Olson et al., 2005). In addition, agonists at μ-opioid, muscarinic or nicotinic cholinergic receptors are all more readily self-administered into the posterior than anterior VTA (Ikemoto and Wise, 2002; Ikemoto et al., 2006; Zangen et al., 2002). The mechanisms underlying these contrasts are unclear, but previous studies might be fruitfully revisited in light of the opposing roles of DA neurons and the RMTg, which overlaps the caudal VTA.

Relation to DA Functions

A pervasive pattern we found in the properties of RMTg neurons was their diametric opposition to reward and motor-activating

functions of DA neurons. RMTg neurons preferentially showed excitations to aversive cues, aversive outcomes, and reward omission, whereas putative DA neurons are preferentially (though not exclusively) inhibited by these same stimuli. RMTg and DA neurons also have opposing effects on motor behavior: RMTg lesions cause mild hyperactivity and marked reductions in fear-induced freezing, whereas DA depletion reduces motor activity and enhances fear-induced freezing (Lenard and Beer, 1975). RMTg lesions also abolished the normal avoidance of the open arms on an elevated plus maze, suggesting that RMTg activation can selectively inhibit discrete behaviors such as arm entry. Again, this is opposite to the hypothesized role for phasic DA release in promoting discrete motivated behaviors, such as individual lever-presses for cocaine (Phillips et al., 2003).

Given the close relationship of RMTg to DA function, it should be recognized that neither population of neurons is homogeneous. Individual VTA DA neurons project to one of many targets (Ikemoto 2007), and DA neurons with different targets have different physiological properties (Margolis et al., 2006, 2008; Ford et al., 2006) and may be activated at different times by different stimuli (Schultz 2007), including aversive stimuli (Feenstra et al., 2001). Because different subsets of DA neurons receive topographic inputs from different subregions of the RMTg (Jhou et al., 2009), these distinct channels of information apparent in DA systems might also be reflected in the RMTg. Such a hypothesis is consistent with numerous physiological differences we saw between the RMTg core and periphery: RMTg core neurons expressed stimuli-induced Fos more avidly than peripheral neurons, were more likely to project to the VTA (versus SNC) and showed particularly fast phasic responses to stimuli. These findings add to previously observed anatomic differences between medial and lateral portions of the RMTg (Jhou et al., 2009). The functional significance of these differences is not yet known, but one attractive hypothesis is that the RMTg's medial and lateral portions preferentially influence VTA (limbic) and SNC (motor) dopamine functions, respectively. For example, the rapid phasic responses in the RMTg core may be particularly suited to carrying the cognitive information required by temporal difference learning models (Montague et al., 1996; Sutton and Barto, 1998), whereas the slower ramping responses in some lateral RMTg units might instead play roles in the more long-lasting motor responses to such stimuli.

The RMTg also sends descending projections to numerous brainstem regions aside from DA neurons. These include projections to the raphe nuclei, PPTg, laterodorsal tegmental nucleus, and locus ceruleus (Jhou et al., 2009), regions which broadly influence attention, cognition, emotion, and motor behavior. RMTg efferents also innervate Barrington's nucleus (Jhou et al., 2009), which modulates micturition, a function with obvious relationships to emotion. Hence, the RMTg may not "merely" modulate DA function, but likely constitutes a distinct system for coordinating responses to negatively valenced stimuli.

Implications for Future Study

The RMTg has only recently been differentiated from surrounding areas, and much remains to be learned about its function. For example, the current study focused on the motor performance effects of the RMTg, but did not examine its roles in learning. Because DA neurons are believed to serve as "teaching" signals mediating learning in downstream targets (Schultz, 2007), we hypothesize that the RMTg may perform a similar but inverted function, i.e., an "aversive teaching signal." Notably, one major afferent to the RMTg arises from the anterior cingulate cortex, which provides just such an aversive teaching signal for avoidance learning (Johansen and Fields, 2004). Other implications of our findings arise from the finding that the RMTg is needed to selectively inhibit entry into open arms on a plus maze, suggesting that phasic RMTg activation might inhibit specific behavioral impulses, with implications for understanding addictions and compulsions, which are characterized by a failure to inhibit specific maladaptive behaviors. Another notable property of the RMTg is its high level of μ-opioid receptor expression (Jhou et al., 2009), suggesting novel mechanisms by which opioids would modulate all of the above functions, including cognitive, motor, and affective elements of aversive behavior.

Finally, our results, along with recent findings from Hikosaka and colleagues, suggest an especially close interaction between regions processing appetitive and aversive affective stimuli. This relationship may lend support to long-standing theoretical ideas regarding opponent processing of affective stimuli (Konorski, 1967; Daw et al., 2002; Fields, 2007; Koob and LeMoal, 2008; Solomon and Corbit, 1974; Matsumoto and Hikosaka, 2007). Current and future studies of the RMTg should therefore contribute to a richer view of motivated behavior as a product of interaction between appetitive and aversive processes, akin to "neuroeconomic" models of decision-making (Phillips et al., 2007).

EXPERIMENTAL PROCEDURES

Animals

All procedures were in accordance with guidelines set by the Animal Care and Use Committees at Johns Hopkins University, Harvard Medical School, and/or Beth Israel Deaconess Medical Center. We used 5 male Sprague-Dawley rats for tracing experiments, 40 for Fos experiments, 16 for electrophysiology experiments, and 47 for lesion experiments.

Tracer or Excitotoxin Injections into the VTA or RMTg

A burr hole was placed in the skull above the target region and a glass pipette (tip diameter 15 μm) was lowered into the brain. The pipette contained either the anterograde tracer biotinylated dextran-amine (BD, Molecular Probes, 12.5% in saline), the retrograde tracer cholera toxin B subunit (CTB, List Biological, 1% in saline), or the excitotoxin ibotenic acid (10% in saline, adjusted to pH 7.4 with NaOH). RMTg coordinates were 7.6 mm caudal to bregma, 1.0 mm lateral to the midline, and 6.6 mm ventral to the dura. VTA coordinates were 5.2 mm caudal to bregma, 0.9 mm lateral to the midline, and 7.9mm ventral to the dura.

Perfusions and Tissue Sectioning

Rats used for tracing and lesion experiments were sacrificed with an overdose of chloral hydrate (350 mg/kg injected intraperitoneally), while rats used for Fos or electrophysiology were sacrificed with an overdose of isoflurane. Rats were perfused transcardially with 10% formalin in 0.1 M phosphate-buffered saline (pH 7.4). Brains from electrophysiology experiments had 4% potassium ferricyanide (Sigma) added to the perfusate, allowing electrode tips to be visualized by passage of 100 μA current just before perfusion. Brains were removed from the skull, equilibrated overnight in 20% sucrose solution, and cut into 40 μm sections on a freezing microtome. Cut sections were stored in phosphate buffered saline (PBS) with 0.05% sodium azide preservative until processed.

Nissl Staining

Brain sections mounted on gelatin-coated slides were dehydrated in graded ethanols (60 s each in 50%, 70%, 95%, and 100% ethanol), then rehydrated and placed into thionin solution (0.25% in 0.2 M sodium acetate buffer [pH 4.5]) for 30 s. Slides were then dehydrated in graded ethanols, with 1% acetic acid added to the 95% ethanol solution to remove background staining. Slides were then placed in xylenes and coverslipped with Permaslip (Alban Scientific, St. Louis, MO).

Stimulus-Induced Fos

Four groups of rats were used to test effects of shocks and shock cues on RMTg Fos, and two groups were used to test food-deprivation and feeding. All rats were habituated to behavioral chambers (Coulbourn Instruments) for 20 min on each of 3 days. On a subsequent test day, the first group ("unstimulated") was placed into the chamber for a 60 min session, then perfused. The second group ("shocked") received four footshocks (0.5 mA, 0.5 s) delivered to the grid floor using a scrambler (Coulbourn Instruments) at 4 min intervals, with the first shock occurring 4 min after placement into the chamber. Rats were perfused 1 hr after the first shock. The third group ("shock-paired cue") received 60 min training sessions on each of 2 consecutive training days, with each session consisting of two 20 s auditory tones (1 kHz, 55 dB) coterminating with a 0.5 mA, 0.5 s footshock. The tone-shock pairs were separated by 20 min intervals, and the first paring occurred 10 min after placement into the chamber. Rats were removed 10 min after the final tone-shock presentation, giving a total session time of 1 hr. One day after training, rats were reacclimated to the chamber for 30 min to reduce possible conditioning of the context to the footshock. On the next day, rats were tested with 8 tones lasting 30 s each, with 60 s between tones. Rats were perfused 1 hr after the session start. The fourth group ("unpaired cue") received two sessions of training in which tone and shock were explicitly unpaired. Training sessions were again 1 hr long, with stimuli presented in the following sequence: tone-shock-tone-shock, with 10 min delays between each stimulus. One day after the second training session, rats were reacclimated to chambers for 30 min, as with the "shock-paired tone" group.

A fifth group ("food deprived") was food deprived to 85% of original body weight, then placed into the behavioral chambers for 1 hr and perfused. The sixth group ("fed") was also deprived to 85% of original body weight, but allowed ad libitum access to a highly palatable sweet food (Froot Loops, Kellogg Co., Battle Creek, MI) for the hour before sacrifice. To avoid neophobic responses, all rats in these two groups were allowed to consume small numbers of Froot Loops for 1–2 days prior to testing.

Immunohistochemistry for Fos Combined with CTB or GAD67

Free-floating sections were immunostained for Fos by overnight incubation in rabbit anti-Fos primary (Ab-5, Calbiochem, raised against amino acids 4–17 of human Fos) at a 1:10,000 dilution in PBS with 0.25% Triton-X and 0.05% sodium azide. Afterwards, tissue was incubated in biotinylated donkey-anti-rabbit secondary (1:1000 dilution, Jackson Immunoresearch, West Grove, PA) for 30 min, followed by six 1 min rinses in PBS, followed by 1 hr in avidin-biotin complex (Vector). Tissue was then rinsed in sodium acetate buffer (0.1 M, pH 7.4), followed by incubation for 5 min in 1% diaminobenzidine (DAB) with nickel and hydrogen peroxide (Vector), revealing a blue-black reaction product. Tissue was rinsed again and incubated overnight in either goat-anti-CTB (1:50,000 dilution, List Biological, Campbell, CA), or mouse-anti-GAD67 (1:20,000 dilution, Chemicon/Millipore) diluted in PBS with 0.05% sodium azide. Afterwards, sections were rinsed in PBS (1 min), incubated 30 min in biotinylated donkey-anti-goat secondary (1:1000, Jackson Immunoresearch), rinsed 6 × 1 min in PBS, incubated 1 hr in avidin-biotin complex, rinsed 2 × 1 min in PBS, and then incubated in 1% DAB with hydrogen peroxide for 10 min, revealing a brown reaction product.

Cell Counts

Fos and/or CTB-labeled neurons were counted in three or four consecutive coronal sections of the RMTg (240 μm spacing between sections). The most rostral section was at the level of the caudal part of the interpeduncular nucleus, while the most caudal section was just rostral to the anterior tegmental nucleus. The RMTg "core" was delineated with a 500 μm radius circle centered medially within the RMTg, where retrograde labeling density was highest. The RMTg "periphery" was delineated with a 1 mm diameter circle centered at the lateral edge of the "core" circle, at all but the most rostral RMTg sections. Fos and/or CTB labeled neurons in the surrounding reticular formation and the overlying PAG were counted in the same coronal sections as in the RMTg. Labeling in the PPTg was counted in three consecutive coronal sections within a 0.5 mm radius circle centered on the superior cerebellar peduncle. Cells in the lateral habenula and lateral hypothalamus were counted in three coronal sections spaced 720 μm apart, in order to span the entire rostrocaudal range of these regions. Cells in the ventral pallidum were counted in a single section where the density of retrograde labeling was highest, while cells in the accumbens shell were counted in three consecutive sections.

Counting of Nissl-stained cells in lesioned animals was performed in photographs taken with a 20× objective, overlaid with a grid template delineating a rectangular region encompassing the RMTg core and diffuse portions (Figures S1 and S2). In this experiment, RMTg cells were counted in five consecutive sections, spaced 160 μm apart. Nissl-stained neurons in the MRN were counted in the same five sections as the RMTg, in a vertical rectangle extending laterally to the borders of the RMTg, dorsally to the ventral edge of the PAG, and ventrally to the pons. Nissl-stained neurons were distinguished from glia by their larger size and labeled cytoplasm.

Behavioral Training for Electrophysiological Recordings

Rats used for recording experiments were water deprived for 24 hr before the first training session. They were then trained to approach a fluid well to receive 50 μl of a 10% sucrose solution after a 70 dB auditory cue (2 kHz tone, white noise, or 20 Hz clicker, counterbalanced). Cue durations in most sessions averaged 2 s, with a range from 1–3 s, at the end of which the reward was delivered if the rat had responded. For some rats, training and testing sessions used cue durations fixed at 2 s. If rats did not respond during the cue, they were allowed indefinite time to respond to receive fluid. New trials began a minimum of 7 s after consuming the previous trial's reward, and a minimum of 15 s after the start of the previous trial, and a minimum of 2 s after any other interruption of the fluid port photobeam. After two shaping sessions, a second distinct cue was introduced (constrained to be the next cue in the tone/noise/clicker series after the cue used for sucrose trials), which also lasted 2 s but was never followed by reward. These "no-reward" trials would time out after 15 s regardless of the rat's behavior. Training continued until rats discriminated between the cues, as evidenced by entering the fluid receptacle on fewer than 5% of "no-reward" cue presentations. This phase of training was used to assess that animals were indeed using auditory cue identities to guide behavior. When criterion was reached, a third cue was introduced (again the next in the tone/noise/clicker series), also 2 s in duration, which was always followed by a brief (20 ms) 0.2 mA footshock that commenced at the auditory cue offset. This third cue was trained for two sessions, during which behavioral suppression to the cue developed extremely rapidly. After this final training session, rats were returned to an ad libitum water schedule before undergoing surgery.

Electrophysiological Recordings

Drivable electrode arrays aimed at the RMTg were implanted at a 10 degree angle to avoid damaging the sagittal sinus, and were implanted dorsally to the RMTg region, allowing electrodes to be lowered progressively through the RMTg after each recording session. Electrode arrays consisted of 25 μm or 50 μm microwires arranged either in a single bundle (Schoenbaum et al., 1999) or in a linear array with a spacing of 250 μm. Wires were attached to a microdrive (modified from Kralik et al., 2001). A ground wire (37 gauge) was implanted into the overlying cortex, and the entire assembly encased in cement (Dentsply International, York PA). Rats were allowed to recover for 7 days, after which the electrode arrays were connected to a unity gain headstage whose output was fed to amplifiers with high-pass and low-pass filter cutoffs of 300 Hz and 9 kHz respectively (Neuralynx, Inc., Bozeman, MT). Rats were recorded for 1–2 sessions per day, and electrodes were advanced 80–160 μm at the end of each session, with at least 2 hr between sessions.

Analysis of Recorded Spikes

During sessions, spike waveforms were digitized at 40 kHz after amplitude thresholding to accept voltage excursions having a 2:1 ratio over background

noise. Waveforms were sorted offline using software that performed principal components analysis (Offline Sorter, Plexon Inc., Dallas, TX). Units were accepted only if a distinct cluster was visible in a 2-D plot of the largest two principal components, if this cluster's location was stable over the duration of the recording session, and if the unit exhibited a well-defined refractory period as defined by fewer than 0.1% of spikes occurring in a 1 ms window after each spike. Perievent spike rates and other parameters were analyzed in Matlab (Mathworks, Natick, MA). Any spikes detected during the brief 20 ms shock period itself were rejected, as these may have been stimulus artifacts from the shocks.

Lesion Effects on Conditioned Freezing

Freezing to an auditory tone was conditioned using parameters similar to those previously described (LaBar and LeDoux, 1996). Rats were exposed to 20 s of an 80 dB tone, the conditioned stimulus (CS), which coterminated with a 1 s 120 dB tone, the aversive unconditioned stimulus (US). Rats were habituated to the testing chamber (Med Associates, St. Albans, VT) for 15 min on each of 2 days prior to testing. On the test day, rats were again habituated for 15 min, then exposed to six consecutive CS-US pairings, with a 2–3 min randomized time interval between stimulus presentations. Freezing was identified as a lack of all movements except those related to respiration. All behaviors were scored prior to histological examination, blinding the observer the lesion size and placement.

Lesion Effects on Unconditioned Freezing

Unconditioned freezing to the predator odor trimethylthiazoline (TMT) was tested in the rat's home cage (dimensions 25 × 48 cm, height 20 cm). Wiretop food racks were retained during testing, along with food, because the reduced ambient volume increased rats' propensity to freeze. To avoid premature exposure of rats to odors, rats were tested individually in a room with reduced air pressure, preventing ventilation into the rest of the animal facility, and at least 24 hr were allotted between sessions to allow odors to dissipate from the room. On the test day, a gauze pad was taped to one end of the cage wall 6 inches above the floor, after which rats were allowed to acclimate for 15 min. Next, we placed 20 μl of water onto the pad for a 10 min baseline period, followed by 20 μl of TMT onto the pad for the 10 min test period. After each placement of liquid, a filter top lid was placed over the cage to reduce ambient airflow, and the experimenter left the room to avoid disrupting behavior, which was recorded on 8 mm videotape. At session end, rats were transferred to a fresh homecage to avoid reintroducing odors to the colony. Behavior was scored prior to histological examination of lesions, effectively blinding the experimenter to lesion extent. Freezing behavior was identified in the same manner as in the tone conditioning tests, while defensive burying behavior was identified by a stereotyped rapid and repetitive forward thrusting of the forepaws, sometimes accompanied by a shoveling motion of the snout.

SUPPLEMENTAL DATA

The Supplemental Data include two figures and can be found with this article online at http://www.neuron.org/supplemental/S0896-6273(09)00121-4.

REFERENCES

Araki, M., McGeer, P.L., and Kimura, H. (1988). The efferent projections of the rat lateral habenular nucleus revealed by the PHA-L anterograde tracing method. Brain Res. *44*, 319–330.

Avanzi, V., Castilho, V.M., de Andrade, T.G., and Brandao, M.L. (1998). Regulation of contextual conditioning by the median raphe nucleus. Brain Res. *790*, 178–184.

Brooks, J., and Tracey, I. (2005). From nociception to pain perception: imaging the spinal and supraspinal pathways. J. Anat. *207*, 19–33.

Christoph, G.R., Leonzio, R.J., and Wilcox, K.S. (1986). Stimulation of the lateral habenula inhibits dopamine-containing neurons in the substantia nigra and ventral tegmental area of the rat. J. Neurosci. *6*, 613–619.

Coizet, V., Dommett, E.J., Redgrave, P., and Overton, P.G. (2006). Nociceptive responses of midbrain dopaminergic neurones are modulated by the superior colliculus in the rat. Neuroscience *139*, 1479–1493.

Colussi-Mas, J., Geisler, S., Zimmer, L., Zahm, D.S., and Bérod, A. (2007). Activation of afferents to the ventral tegmental area in response to acute amphetamine: a double-labelling study. Eur. J. Neurosci. *26*, 1011–1025.

Daw, N.D., Kakade, S., and Dayan, P. (2002). Opponent interactions between serotonin and dopamine. Neural Netw. *15*, 603–616.

Dickinson, A., and Dearing, M.F. (1979). Appetitive-aversive interactions and inhibitory processes. In Mechanisms of Learning and Motivation, A. Dickinson and R.A. Boakes, eds. (Hillsdale, NJ: Erlbaum), pp. 203–231.

Feenstra, M.G., Vogel, M., Botterblom, M.H., Joosten, R.N., and de Bruin, J.P. (2001). Dopamine and noradrenaline efflux in the rat prefrontal cortex after classical aversive conditioning to an auditory cue. Eur. J. Neurosci. *13*, 1051–1054.

Fendt, M., Endres, T., and Apfelbach, R. (2003). Temporary inactivation of the bed nucleus of the stria terminalis but not of the amygdala blocks freezing induced by trimethylthiazoline, a component of fox feces. J. Neurosci. *23*, 23–28.

Ferreira, J.G., Del-Fava, F., Hasue, R.H., and Shammah-Lagnado, S.J. (2008). Organization of ventral tegmental area projections to the ventral tegmental area-nigral complex in the rat. Neuroscience *153*, 196–221.

Fields, H.L. (2007). Understanding how opioids contribute to reward and analgesia. Reg Anesth Pain Med. *32*, 242–246.

Ford, C.P., Mark, G.P., and Williams, J.T. (2006). Properties and opioid inhibition of mesolimbic dopamine neurons vary according to target location. J. Neurosci. *26*, 2788–2797.

Geisler, S., and Zahm, D.S. (2005). Afferents of the ventral tegmental area in the rat—anatomical substratum for integrative functions. J. Comp. Neurol. *490*, 270–294.

Geisler, S., and Trimble, M. (2008). The lateral habenula: no longer neglected. CNS Spectr. *13*, 484–489.

Geisler, S., Marinelli, M., Degarmo, B., Becker, M.L., Freiman, A.J., Beales, M., Meredith, G.E., and Zahm, D.S. (2008). Prominent activation of brainstem and pallidal afferents of the ventral tegmental area by cocaine. Neuropsychopharmacology *33*, 2688–2700.

Heldt, S.A., and Ressler, K.J. (2006). Lesions of the habenula produce stress- and dopamine-dependent alterations in prepulse inhibition and locomotion. Brain Res. *1073–1074*, 229–239.

Herkenham, M., and Nauta, W.J. (1979). Efferent connections of the habenular nuclei in the rat. J. Comp. Neurol. *187*, 19–47.

Hikosaka, O., Sesack, S., Lecourtier, L., and Shepard, P. (2008). Habenula: crossroad between the basal ganglia and the limbic system. J. Neurosci. *28*, 11825–11829.

Hollerman, J.R., and Schultz, W. (1998). Dopamine neurons report an error in the temporal prediction of reward during learning. Nat. Neurosci. *1*, 304–309.

Holstege, G. (1991). Descending motor pathways and the spinal motor system: limbic and non-limbic components. Prog. Brain Res. 87, 307–421.

Holstege, G., Meiners, L., and Tan, K. (1985). Projections of the bed nucleus of the stria terminalis to the mesencephalon, pons, and medulla oblongata in the cat. Exp. Brain Res. 58, 379–391.

Hopkins, D.A., and Holstege, G. (1978). Amygdaloid projections to the mesencephalon, pons and medulla oblongata in the cat. Exp. Brain Res. 32, 529–547.

Ikemoto, S. (2007). Dopamine reward circuitry: two projection systems from the ventral midbrain to the nucleus accumbens-olfactory tubercle complex. Brain Res. Rev. 56, 27–78.

Ikemoto, S., and Wise, R.A. (2002). Rewarding effects of the cholinergic agents carbachol and neostigmine in the posterior ventral tegmental area. J. Neurosci. 22, 9895–9904.

Ikemoto, S., Murphy, J.M., and McBride, W.J. (1997). Self-infusion of GABA(A) antagonists directly into the ventral tegmental area and adjacent regions. Behav. Neurosci. 111, 369–380.

Ikemoto, S., Murphy, J.M., and McBride, W.J. (1998). Regional differences within the rat ventral tegmental area for muscimol self-infusions. Pharmacol. Biochem. Behav. 61, 87–92.

Ikemoto, S., Qin, M., and Liu, Z.H. (2006). Primary reinforcing effects of nicotine are triggered from multiple regions both inside and outside the ventral tegmental area. J. Neurosci. 26, 723–730.

Jhou, T. (2005). Neural mechanisms of freezing and passive aversive behaviors. J. Comp. Neurol. 493, 111–114.

Jhou, T.C., Geisler, S., Marinelli, M., DeGarmo, B., and Zahm, D.S. (2009). The mesopontine rostromedial tegmental nucleus: a structure targeted by the lateral habenula that projects to the ventral tegmental area of Tsai and substantia nigra compacta. J. Comp. Neurol. 513, 566–596.

Ji, H., and Shepard, P.D. (2007). Lateral habenula stimulation inhibits rat midbrain dopamine neurons through a GABA(A) receptor-mediated mechanism. J. Neurosci. 27, 6923–6930.

Johansen, J.P., and Fields, H.L. (2004). Glutamatergic activation of anterior cingulate cortex produces an aversive teaching signal. Nat. Neurosci. 7, 398–403.

Kaufling, J., Veinante, P., Pawlowski, S.A., Freund-Mercier, M.-J., and Barrot, M. (2009). Afferents to the GABAergic tail of the ventral tegmental area in the rat. J. Comp. Neurol. 513, 597–621.

Kim, J.J., Rison, R.A., and Fanselow, M.S. (1993). Effects of amygdala, hippocampus, and periaqueductal gray lesions on short- and long-term contextual fear. Behav. Neurosci. 107, 1093–1098.

Konorski, J. (1967). Integrative Activity of the Brain: An Interdisciplinary Approach (Chicago: University of Chicago Press).

Koob, G.F., and Le Moal, M. (2008). Addiction and the brain antireward system. Annu. Rev. Psychol. 59, 29–53.

Kralik, J.D., Dimitrov, D.F., Krupa, D.J., Katz, D.B., Cohen, D., and Nicolelis, M.A. (2001). Techniques for long-term multisite neuronal ensemble recordings in behaving animals. Methods 25, 121–150.

LaBar, K.S., and LeDoux, J.E. (1996). Partial disruption of fear conditioning in rats with unilateral amygdala damage: correspondence with unilateral temporal lobectomy in humans. Behav. Neurosci. 110, 991–997.

Lecourtier, L., and Kelly, P.H. (2005). Bilateral lesions of the habenula induce attentional disturbances in rats. Neuropsychopharmacology 30, 484–496.

LeDoux, J.E., Iwata, J., Cicchetti, P., and Reis, D.J. (1988). Different projections of the central amygdaloid nucleus mediate autonomic and behavioral correlates of conditioned fear. J. Neurosci. 8, 2517–2529.

Lee, J.L., Dickinson, A., and Everitt, B.J. (2005). Conditioned suppression and freezing as measures of aversive Pavlovian conditioning: effects of discrete amygdala lesions and overtraining. Behav. Brain Res. 159, 221–233.

Leknes, S., and Tracey, I. (2008). A common neurobiology for pain and pleasure. Nat. Rev. Neurosci. 9, 314–320.

Lenard, L.G., and Beer, B. (1975). 6-Hydroxydopamine and avoidance: Possible role of response suppression. Pharmacol. Biochem. Behav. 3, 873–878.

Margolis, E.B., Lock, H., Chefer, V.I., Shippenberg, T.S., Hjelmstad, G.O., and Fields, H.L. (2006). Kappa opioids selectively control dopaminergic neurons projecting to the prefrontal cortex. Proc. Natl. Acad. Sci. USA 103, 2938–2942.

Margolis, E.B., Mitchell, J.M., Ishikawa, J., Hjelmstad, G.O., and Fields, H.L. (2008). Midbrain dopamine neurons: projection target determines action potential duration and dopamine D(2) receptor inhibition. J. Neurosci. 28, 8908–8913.

Matsumoto, M., and Hikosaka, O. (2007). Lateral habenula as a source of negative reward signals in dopamine neurons. Nature 447, 1111–1115.

Matsumoto, M., and Hikosaka, O. (2009). Representation of negative motivational value in the primate lateral habenula. Nat. Neurosci. 12, 77–84.

McNally, G.P., and Westbrook, R.F. (2006). Predicting danger: the nature, consequences, and neural mechanisms of predictive fear learning. Learn. Mem. 13, 245–253.

Mirenowicz, J., and Schultz, W. (1994). Importance of unpredictability for reward responses in primate dopamine neurons. J. Neurophysiol. 72, 1024–1027.

Mirenowicz, J., and Schultz, W. (1996). Preferential activation of midbrain dopamine neurons by appetitive rather than aversive stimuli. Nature 379, 449–451.

Montague, P.R., Dayan, P., and Sejnowski, T.J. (1996). A framework for mesencephalic dopamine systems based on predictive Hebbian learning. J. Neurosci. 16, 1936–1947.

Müller, M., and Fendt, M. (2006). Temporary inactivation of the medial and basolateral amygdala differentially affects TMT-induced fear behavior in rats. Behav. Brain Res. 167, 57–62.

Murphy, C.A., DiCamillo, A.M., Haun, F., and Murray, M. (1996). Lesion of the habenular efferent pathway produces anxiety and locomotor hyperactivity in rats: a comparison of the effects of neonatal and adult lesions. Behav. Brain Res. 81, 43–52.

Olson, V.G., and Nestler, E.J. (2007). Topographical organization of GABAergic neurons within the ventral tegmental area of the rat. Synapse 61, 87–95.

Olson, V.G., Zabetian, C.P., Bolanos, C.A., Edwards, S., Barrot, M., Eisch, A.J., Hughes, T., Self, D.W., Neve, R.L., and Nestler, E.J. (2005). Regulation of drug reward by cAMP response element-binding protein: evidence for two functionally distinct subregions of the ventral tegmental area. J. Neurosci. 25, 5553–5562.

Owings, D.H., and Morton, E.S. (1998). Animal Vocal Communication: A New Approach (Cambridge: Cambridge University Press).

Pan, W.X., Schmidt, R., Wickens, J.R., and Hyland, B.I. (2005). Dopamine cells respond to predicted events during classical conditioning: evidence for eligibility traces in the reward-learning network. J. Neurosci. 25, 6235–6242.

Paton, J.J., Belova, M.A., Morrison, S.E., and Salzman, C.D. (2006). The primate amygdala represents the positive and negative value of visual stimuli during learning. Nature 439, 865–870.

Perrotti, L.I., Bolaños, C.A., Choi, K.H., Russo, S.J., Edwards, S., Ulery, P.G., Wallace, D.L., Self, D.W., Nestler, E.J., and Barrot, M. (2005). DeltaFosB accumulates in a GABAergic cell population in the posterior tail of the ventral tegmental area after psychostimulant treatment. Eur. J. Neurosci. 21, 2817–2824.

Pezuk, P., Aydin, E., Aksoy, A., and Canbeyli, R. (2008). Effects of BNST lesions in female rats on forced swimming and navigational learning. Brain Res. 1228, 199–207.

Phillips, P.E., Stuber, G.D., Heien, M.L., Wightman, R.M., and Carelli, R.M. (2003). Subsecond dopamine release promotes cocaine seeking. Nature 422, 614–618.

Phillips, P.E., Walton, M.E., and Jhou, T.C. (2007). Calculating utility: preclinical evidence for cost-benefit analysis by mesolimbic dopamine. Psychopharmacology (Berl.) 191, 483–495.

Reynolds, S.M., and Berridge, K.C. (2001). Fear and feeding in the nucleus accumbens shell: rostrocaudal segregation of GABA-elicited defensive behavior versus eating behavior. J. Neurosci. 21, 3261–3270.

Saddoris, M.P., Gallagher, M., and Schoenbaum, G. (2005). Rapid associative encoding in basolateral amygdala depends on connections with orbitofrontal cortex. Neuron 46, 321–331.

Scammell, T.E., Estabrooke, I.V., McCarthy, M.T., Chemelli, R.M., Yanagisawa, M., Miller, M.S., and Saper, C.B. (2000). Hypothalamic arousal regions are activated during modafinil-induced wakefulness. J. Neurosci. 20, 8620–8628.

Schoenbaum, G., Chiba, A.A., and Gallagher, M. (1999). Neural encoding in orbitofrontal cortex and basolateral amygdala during olfactory discrimination learning. J. Neurosci. 19, 1876–1884.

Schultz, W. (2007). Multiple dopamine functions at different time courses. Annu. Rev. Neurosci. 30, 259–288.

Schulz, D., and Canbeyli, R.S. (2000). Lesion of the bed nucleus of the stria terminalis enhances learned despair. Brain Res. Bull. 52, 83–87.

Solomon, R.L., and Corbit, J.D. (1974). An opponent-process theory of motivation. I. Temporal dynamics of affect. Psychol. Rev. 81, 119–145.

Sparks, P.D., and LeDoux, J.E. (1995). Septal lesions potentiate freezing behavior to contextual but not to phasic conditioned stimuli in rats. Behav. Neurosci. 109, 184–188.

Sutton, R.S., and Barto, A.G. (1998). Reinforcement Learning, an Introduction (Cambridge, MA: MIT Press).

Swerdlow, N.R., Koob, G.F., Cador, M., Lorang, M., and Hauger, R.L. (1993). Pituitary-adrenal axis responses to acute amphetamine in the rat. Pharmacol. Biochem. Behav. 45, 629–637.

Tepper, J.M., and Lee, C.R. (2007). GABAergic control of substantia nigra dopaminergic neurons. Prog. Brain Res. 160, 189–208.

Treit, D., and Menard, J. (1997). Dissociations among the anxiolytic effects of septal, hippocampal, and amygdaloid lesions. Behav. Neurosci. 111, 653–658.

Treit, D., and Pinel, J.J.P. (2005). Defensive Burying. In The Behavior of the Laboratory Rat, a Handbook with Tests, I.Q. Whishaw and B. Kolb, eds. (Oxford: Oxford University Press).

Ungless, M.A., Magill, P.J., and Bolam, J.P. (2004). Uniform inhibition of dopamine neurons in the ventral tegmental area by aversive stimuli. Science 303, 2040–2042.

Wirtshafter, D., and Trifunovic, R. (1992). Nonserotonergic control of nucleus accumbens dopamine metabolism by the median raphe nucleus. Pharmacol. Biochem. Behav. 41, 501–505.

Zangen, A., Ikemoto, S., Zadina, J.E., and Wise, R.A. (2002). Rewarding and psychomotor stimulant effects of endomorphin-1: anteroposterior differences within the ventral tegmental area and lack of effect in nucleus accumbens. J. Neurosci. 22, 7225–7233.